Enhancement of the Thermoelectric Figure of Merit in n-type Cu$_{0.008}$Bi$_2$Te$_{2.7}$Se$_{0.3}$ by Using Nb Doping

Kyu Hyoung Lee

Department of Nano Applied Engineering, Kangwon National University, Chuncheon 24341, Korea

Byungki Ryu

Korea Electrotechnology Research Institute, Changwon 51543, Korea

Hee Jung Park

Advanced Materials Engineering, Daejeon University, Daejeon 34520, Korea

Kimoon Lee

Department of Physics, Kunsan National University, Kunsan 54150, Korea

Jong Wook Roh, Sang Il Kim and Sungwoo Hwang*

Materials R&D Center, Samsung Advanced Institute of Technology, Suwon 16678, Korea

Soon-Mok Choi

School of Energy, Materials and Chemical Engineering,
Korea University of Technology and Education, Cheonan 31253, Korea

Jong-Young Kim

Icheon branch, Korea Institute of Ceramic Engineering and Technology, Icheon 17303, Korea

Jeong Hoon Lee

Department of Electrical Engineering, Kwangwoon University, Seoul 01897, Korea

Jae-Hong Lim

Electrochemistry Department, Korea Institute of Materials Science, Changwon 51508, Korea

Sung Wng Kim

Department of Energy Science, Sungkyunkwan University, Suwon 16419, Korea

Doping with foreign atom has been shown to be an effective way to enhance the dimensionless figure of merit ZT of Bi$_2$Te$_3$-based thermoelectric raw materials. Herein, we report that doping with Nb is effective in enhancing the Seebeck coefficient of n-type Cu$_{0.008}$Bi$_2$Te$_{2.7}$Se$_{0.3}$ polycrystalline bulks. Considering compensation of the Seebeck coefficient due to decrease of the electrical conductivity in Nb-doped compositions, the absolute value of Seebeck coefficient rather increased benefiting from an enhancement of the density of states (DOS) effective mass m^* from $1.09m_0$ (Cu$_{0.008}$Bi$_2$Te$_{2.7}$Se$_{0.3}$) to $1.21m_0 - 1.27m_0$ (Cu$_{0.008}$Bi$_{2-x}$Nb$_x$Te$_{2.7}$Se$_{0.3}$) due to a DOS engineering effect. The values of ZT were 0.84 at 300 K and 0.86 at 320 K for Cu$_{0.008}$Bi$_{1.99}$Nb$_{0.01}$Te$_{2.7}$Se$_{0.3}$. This compositional tuning approach highlights the possibility of further enhancement of ZT for n-type Bi$_2$Te$_3$-based compounds by using a combination of nanostructuring technologies to reduce the thermal conductivity.

I. INTRODUCTION

Thermoelectric (TE) materials have been intensively investigated to realize highly efficient power generation and eco-friendly cooling systems. Among TE materials, Bi_2Te_3-based alloys are widely used for small-scale cooling and refrigerating applications due to their high TE conversion efficiency, which is evaluated by using the dimensionless figure of merit ZT ($= \sigma S^2 T/\kappa$, where σ is the electrical conductivity, S is the Seebeck coefficient, and κ is the total thermal conductivity at a given absolute temperature T), at temperatures near room temperature. The maximum ZT values of commercialized Bi_2Te_3-based ingots are about 1.0 both for p-type ($Bi_{2-x}Sb_xTe_3$) and n-type ($Bi_2Te_{3-y}Se_y$) materials; however, wider applications including automobile TE power generation (ATEG) are limited because of low ZT value and poor mechanical properties.

For p-type $Bi_{2-x}Sb_xTe_3$-based materials, the TE performance and the mechanical properties have been remarkably enhanced by the fabrication of nanostructured polycrystalline bulks. The value of ZT was increased by $40 - 50\%$ ($ZT_{max} \sim 1.5$ at 300 K) [1], and the bending strength was greatly improved by 800% (~ 80 MPa) [2] as compared with a commercial zone-melted ingot. These materials were fabricated via high energy ball-milling or a rapid solidification process (melt spinning or spark erosion) combined with pressure-induced sintering techniques such as hot-pressing and spark plasma sintering (SPS) [1,3,4]. Enhanced mechanical properties could also be obtained in n-type $Bi_2Te_{3-y}Se_y$-based materials by the fabrication of polycrystalline bulks; however, uncontrollable formation of point defects (antisite defects and vacancies) during the powder metallurgical processes caused a severe reproducibility issue [5]. This reproducibility problem in polycrystalline n-type $Bi_2Te_{2.7}Se_{0.3}$ has been improved through the intercalation of a small number of Cu atoms, which suppressed the escape of Te atoms, and a high ZT of 0.9 was observed at 300 K in a $Cu_{0.01}Bi_2Te_{2.7}Se_{0.3}$ nanocomposite fabricated by using high-energy ball milling and hot pressing due to the synergetic effect of the enhanced carrier mobility (μ) and the reduced lattice thermal conductivity (κ_{lat}) [5]. Very recently, we demonstrated the Cu intercalation effect for reproducibility in SPSed bulks with a micro-grain structure. The enhanced ZT of 0.73 with high reproducibility was obtained in $Cu_{0.008}Bi_2Te_{2.7}Se_{0.3}$ at 300 K [6]. Compared to $Bi_2Te_{2.7}Se_{0.3}$, the ZT value was increased by more than 15%; however, this ZT value of an n-type material is still too low compared with that for its p-type counterparts. Doping with foreign atoms is one of the most promising approaches for ZT enhancement because the power factor (σS^2) can be increased by forming a large density of states (DOS) [7–10], and/or the lat can be reduced by intensified point-defect

*E-mail: ledsopp.hwang@samsung.com; Fax: +82-31-8061-1089

phonon scattering [11]. In the present study, we selected $Cu_{0.008}Bi_2Te_{2.7}Se_{0.3}$ as a reference material and achieved an enhancement in S by controlling the doping of Nb at the Bi-site. The theoretical and the experimental analyses for the electronic and the thermal transport properties are discussed to clarify the effect of Nb doping on the TE properties.

II. EXPERIMENTS

We prepared ingots of $Cu_{0.008}Bi_2Te_{2.7}Se_{0.3}$ (CBTS) and Nb-doped CBTS ($Cu_{0.008}Bi_{2-x}Nb_xTe_{2.7}Se_{0.3}$, $x = 0.005, 0.01, 0.02$) by using high-purity elemental Bi (99.999%, 5N Plus), Nb (99.99%, CERAC), Te (99.999%, 5N Plus), and Se (99.999%, 5N Plus) as starting materials. The elements in stoichiometric amounts were put into a carbon-coated quartz tube (inner diameter ~ 14 mm) and melted in a box furnace for 10 h at 1423 K. The ingots acquired by water quenching were pulverized by using a ball mill for 5 min, and bulk samples were fabricated by SPS technique at 500 °C and 30 MPa for 2 min in a dynamic vacuum chamber (10 mm in diameter and 13 mm in thickness). The relative densities of the SPSed bulks ranged from 7.51 g·cm^{-3} to 7.55 g·cm^{-3} ($> 96\%$ of the theoretical density). Because of the anisotropic characteristics of the TE properties of Bi_2Te_3-based materials, we measured σ, S, and κ in the same direction (perpendicular to the SPS press direction). Disk-shaped samples (10 mm in diameter and 1 mm in thickness) for thermal diffusivity measurements and bar-shaped samples (2 mm $\times$ 2 mm $\times$ 8 mm) for σ and S measurements were cut on planes parallel and perpendicular to the SPS press direction, respectively. The electronic transport properties σ and S were measured at temperatures from 300 K to 480 K using a ZEM-3 system (Seebeck Coefficient/Electrical Resistance Measuring System, ULVAC-RICO, Japan) in a He atmosphere. Hall effect measurements were carried out at 300 K in the van der Pauw configuration under a constant magnetic field (1 T). The μ and the carrier concentration (n_c) were calculated by using a one-band model. The κ values ($= \rho_s \cap C_p \cdot \lambda$) were calculated by measuring the sample's density (ρ_s), heat capacity (C_p), and thermal diffusivity (λ). The C_p values at T > 280 K of all samples were almost constant at 0.155 J·g^{-1}·K^{-1}. Temperature dependence of λ was measured by using a TC-9000 system (Laser Flash Method Thermal Constants Analyzer, ULVAC-RICO, Japan).

III. RESULTS AND DISCUSSION

We fabricated Nb-doped CBTS polycrystalline bulks and evaluated their TE properties expecting that such doping would affect the DOS and, thus, an enhancement of the electronic transport properties might be realized. Figure 1 shows the measured σ, S, and power
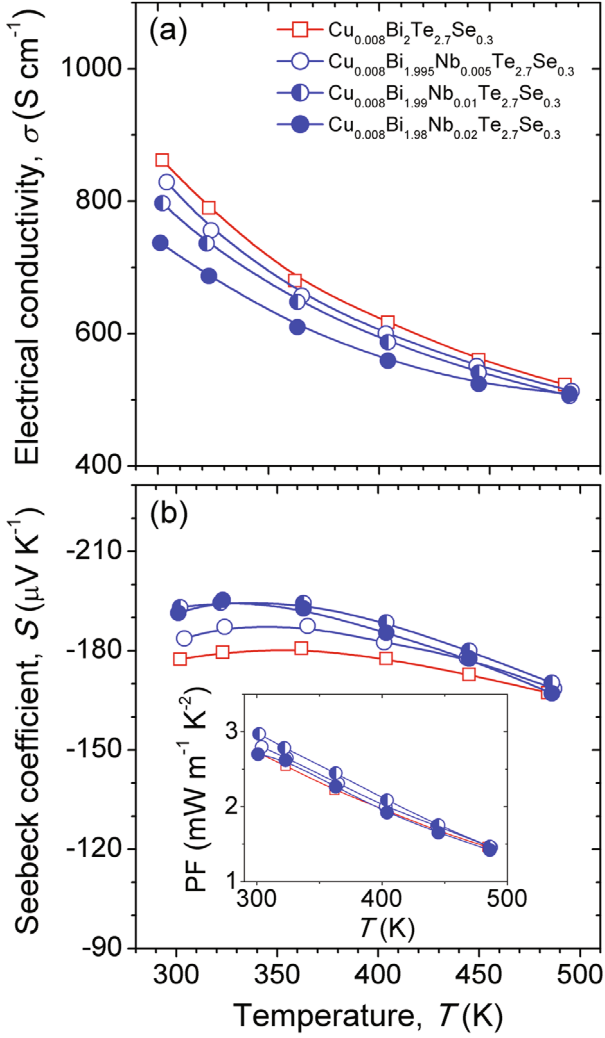
Fig. 1. (Color online) Temperature dependences of (a) the electrical conductivity (σ) and (b) the Seebeck coefficient (S) for CBTS and Nb-doepd CBTS. The calculated power factor is shown in the inset of (b).
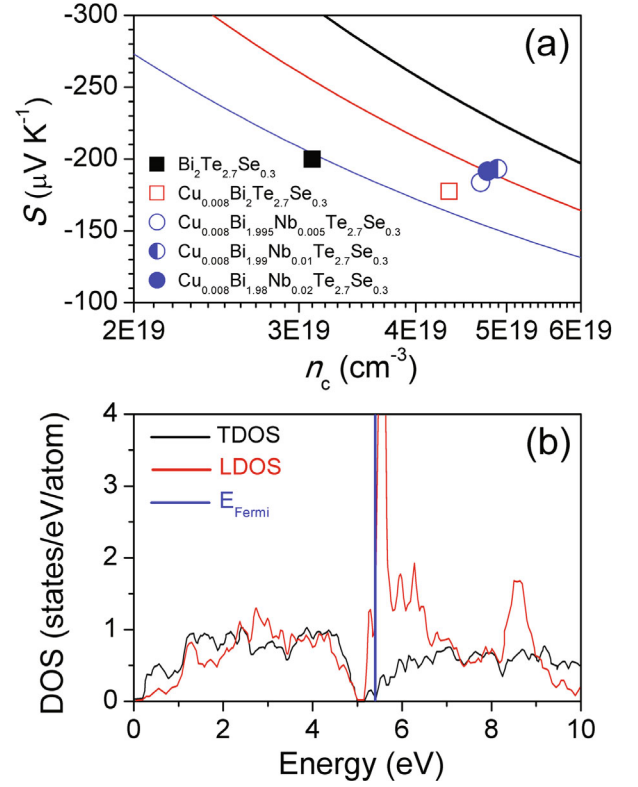

Fig. 2. (Color online) (a) Seebeck coefficient (S) as a function of carrier concentration (n_c) for CBTS and Nb-doped CBTS at 300 K. (b) The electronic density of states (DOS) for Nb-doped BTS. The total DOS (TDOS) of Nb-doped BTS is denoted by the black line, and the local DOS (LDOS) of substitutional Nb is shown by the red line. The solid lines in (a) indicate the Seebeck coefficient calculated with the DOS effective mass (m^*).

factor values of Nb-doped CBTS samples. A reference CBTS sample is also represented for comparison. The values of σ slightly decreased with increased Nb doping (Fig. 1(a)). To elucidate this, we measured the n_c values of CBTS and Nb-doped CBTS at 300 K. The n_c value of CBTS (4.34×10^{19} cm^{-3}) was slightly increased by Nb doping (4.69×10^{19} cm^{-3} for $Cu_{0.008}Bi_{1.995}Nb_{0.005}Te_{2.7}Se_{0.3}$, 4.89×10^{19} cm^{-3} for $Cu_{0.008}Bi_{1.99}Nb_{0.01}Te_{2.7}Se_{0.3}$, and 4.77×10^{19} cm^{-3} for $Cu_{0.008}Bi_{1.98}Nb_{0.02}Te_{2.7}Se_{0.3}$). This is considered to be related with the charge modulation caused by Nb doping. Group 5 elements such as V, Nb, Ta doped on the Bi site might act as electron donors due to their four or five valence electrons, which ahould result in an increased n_c. On the other hand, the μ value of CBTS ($\sim$124 cm^2 V^{-1}s^{-1}) decreased with Nb content ($\sim$110 cm^{2}V^{-1}s^{-1} for $Cu_{0.008}Bi_{1.995}Nb_{0.005}Te_{2.7}Se_{0.3}$, $\sim$102 cm^{2}V^{-1}s^{-1} for $Cu_{0.008}Bi_{1.995}Nb_{0.005}Te_{2.7}Se_{0.3}$, and $\sim$96 cm^{2}V^{-1}s^{-1} for $Cu_{0.008}Bi_{1.995}Nb_{0.005}Te_{2.7}Se_{0.3}$). Thus, the decrease of in Nb-doped CBTS might be due to a reduction in μcaused by electron carrier scattering due to presence of Nb at the Bi sites. Figure 1(b) shows the temperature dependence of S for CBTS and Nb-doped CBTS. One should note that the increase in the value of S for Nb-doped CBTS is rather drastic considering trade-off between and S. This is clearly seen in the plot of the power factor shown in the inset of Fig. 1(b). Despite a decrease in σ, higher power factors were obtained in Nb-doped CBTS, suggesting that the electronic transport properties were enhanced by doping with Nb. The maximum power factor of 2.97 mW m^{-1}K^{-2} was obtained for 0.5 at.% Nb-doped CBTS ($Cu_{0.008}Bi_{1.99}Nb_{0.01}Te_{2.7}Se_{0.3}$) despite the value of its σ (797 S cm^{-1}) being relatively lower than that of CBTS (862 S cm^{-1}).

To clarify the variation of electronic transport behavior in Nb-doped CBTS, we calculated the DOS effective mass m^* and the results are shown in Fig. 2(a). The m^* was estimated from the measured S and n_c with the use
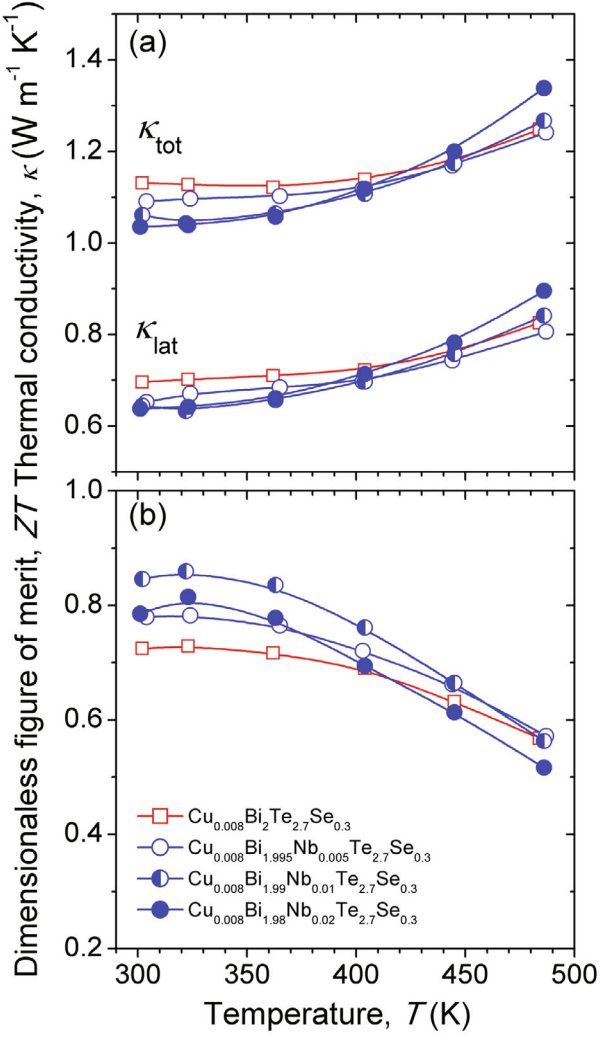
Fig. 3. (Color online) Temperature dependences of (a) the thermal conductivity (κ) and the lattice thermal conductivity (κ_{lat}) and (b) the dimensionless figure of merit ZT for CBTS and Nb-doped CBTS.

of Eq. (1) [12]

$$S = \frac{8\pi^2 k_B^2}{3eh^2}\left(\frac{\pi}{3n_c}\right)^{2/3} m^* T, \tag{1}$$

where k_B, e, and h are the Boltzmann constant, the elementary charge, and the Planck constant, respectively. Figure 2(a) shows the measured S as a function of n_c (Pisarenko plot) for all samples at 300 K. The solid lines are calculated for $m^* = 1.00$, 1.25, and $1.50m)0$ by using Eq. (1), assuming a single parabolic band and an energy-independent carrier-scattering approximation for degenerated semiconductors. As shown in Fig. 2(a), m^* is increased from $1.09m_0$ to $1.21m_0 - 1.27m_0$ by Nb doping. The large m^* values for Nb-doped CBTS are considered to be due to a modification of the electronic structure and could be responsible for the large S. First-principles calculations were performed within density-functional framework to understand the effect of Nb-doping in $Bi_2(Te,Se)_3$ (BTS) [13]. We used the planewave basis, the generalized gradient approximations parameterized by Perdew-Burke-Ernzerhof, and the projector-augmented wave pseudopotentials implemented in the VASP code. For the model structure of BTS, we used a (4×4) unit cell with one quintuple layer containing 32 Bi, 36 Te, and 12 Se atoms. The interaction between Nb and Cu atoms was neglected in our calculations. Our calculations revealed that Nb atoms were stabilized at Bi sites (Nb_{Bi}). Next, we examined the electrical properties in the presence of Nb_{Bi}. Nb_{Bi} impurities form additional levels near the conduction band minimum, as shown in Fig. 2(b). This sharp DOS formation near the Fermi level due to doping of Nb into the BTS system may be the reason for the enhancement of m^* that results in the improvement of S. The formation of an impurity level of Nb_{Bi} is also responsible for a decrease in σ because this may act as a scattering center for an electron carrier.

The κ values of the CBTS and the Nb-doped CBTS samples are shown in Fig. 3(a). The κ values of CBTS were slightly decreased in all Nb-doped samples. We calculated the κ_{lat} values in order to elucidate the point-defect phonon scattering effect caused by the substituted Nb atoms (Fig. 3(a)). The value of κ_{lat} was calculated by subtraction of κ_{ele} from ($\kappa_{lat} = -\kappa_{ele}$), where the electronic contribution κ_{ele} was estimated by using the Wiedemann-Franz law ($\kappa_{ele} = L_0 \cdot T \cdot \sigma$). The Lorenz number L_0 was estimated using following equation:

$$L_0 = \left(\frac{k_B}{e}\right)^2 \left(\frac{(r+7/2)F_{r+5/2}(\eta)}{(r+3/2)F_{r+1/2}(\eta)} - \left[\frac{(r+5/2)F_{r+3/2}(\eta)}{(r+3/2)F_{r+1/2}(\eta)}\right]^2\right), \tag{2}$$

where r is the scattering parameter, $F_n(\eta)$ is the n-th order Fermi integral, and η is Fermi energy. Details of the L_0 calculation have been described elsewhere [14]. The values of L_0 at 300 K, ranging from 1.67×10^{-8} V^2K^{-2}

to 1.79×10^{-8} V^2K^{-2}, were found for the CBTS and the Nb-doped CBTS samples. Although the calculated lat values also included the contribution from bipolar thermal conduction, those of the Nb-doped CBTS samples at

low temperatures (< 400 K) were slightly decreased due to the intensified point-defect phonon scattering caused by the mass difference between the host ion ($M_{Bi} = 209.0$) and the dopant ($M_{Nb} = 92.9$). On the other hand, the behavior of the temperature dependence of κ changed with Nb doping. A steeper increase in κ with increasing in temperature was observed in Nb-doped CBTS due to bipoar thermal conduction.

Figure 3(b) presents the temperature dependences of ZT for CBTS and Nb-doped CBTS. The ZT value was largely enhanced by Nb-doping especially at low temperatures (< 360 K). The highest ZT value obtained was 0.86 at 320 K for the $Cu_{0.008}Bi_{1.98}Nb_{0.02}Te_{2.7}Se_{0.3}$ sample, which is about 18% higher than that of the reference CBTS ($ZT = 0.73$ at 320 K). Although the κ_{lat} values were not decreased by doping with Nb, the value of ZT was increased due to the enhancement in S that originated from the DOS engineering effect.

IV. CONCLUSION

Polycrystalline bulk samples of Nb-doped $Cu_{0.008}Bi_2Te_{2.7}Se_{0.3}$ were fabricated by using spark plasma sintering technique. We experimentally showed an enhancement of the thermoelectric performance of n-type Cu-intercalated Bi-Te-Se systems. The Seebeck coefficient ahowed a significant increase that originated from the enlarged density of states effective mass, as a result of density of states engineering in the formation of the resonant state. Additionally, the lattice thermal conductivity was reduced by point-defect phonon scattering in the presence of Nb at the Bi site. Thus, an enhanced thermoelectric performance ($ZT = 0.86$ at 320 K) was obtained for $Cu_{0.008}Bi_{1.99}Nb_{0.01}Te_{2.7}Se_{0.3}$.

REFERENCES

[1] W. Xie, X. Tang, Y. Yan, Q. Zhang and T. M. Tritt, Appl. Phys. Lett. **94**, 102111 (2009).
[2] J. Jiang, L. Chen, S. Bai, Q. Yao and Q. Wang, Scripta Mater. **52**, 347 (2005).
[3] B. Poudel *et al.*, Science **320**, 634 (2008).
[4] P. K. Nguyen *et al.*, Nanotechnology **23**, 415604 (2012).
[5] W. Liu *et al.*, Adv. Energy Mater. **1**, 577 (2011).
[6] K. H. Lee *et al.*, Current Applied Physics, in press.
[7] H. Y. Lv, H. J. Liu, L. Pan, Y. W. Wen, X. J. Tan, J. Shi and X. F. Tang, Appl. Phys. Lett. **96**, 142101 (2010).
[8] M. Liu, X. Y. Qin, C. S. Liu and Z. Zeng, Appl. Phys. Lett. **99**, 062112 (2011).
[9] H. J. Goldsmid, J. Electron. Mater. **41**, 2126 (2012).
[10] Y. Takagiwa, Y. Pei, G. Pomrehn and G. J. snyder, Appl. Phys. Lett. **101**, 092102 (2012).
[11] H. J. Goldsmid, J. Appl. Phys. **32**, 2198 (1961).
[12] G. J. Snyder and E. S. Toberer, Nat. Mater. **7**, 105 (2008).
[13] P. Hohenberg and W. Kohn, Phys. Rev. **136**, B864 (1964).
[14] L. Zhao *et al.*, J. Am. Chem. Soc. **133**, 20476 (2011).